

PAPER • OPEN ACCESS

## Comparison of inflow-turbulence and trailing-edge noise models with measurements of a 200-kW vertical axis wind turbine

To cite this article: E. Möllerström and F. Ottermo 2019 *J. Phys.: Conf. Ser.* **1222** 012028

View the [article online](#) for updates and enhancements.



**IOP | ebooks™**

Bringing you innovative digital publishing with leading voices to create your essential collection of books in STEM research.

Start exploring the collection - download the first chapter of every title for free.

# Comparison of inflow-turbulence and trailing-edge noise models with measurements of a 200-kW vertical axis wind turbine

E. Möllerström<sup>1</sup> and F. Ottermo<sup>1</sup>

<sup>1</sup> The Rydberg Laboratory for Applied Sciences, Halmstad University, PO Box 823, SE-301 18 Halmstad, Sweden

E-mail: [erik.mollerstrom@hh.se](mailto:erik.mollerstrom@hh.se)

**Abstract.** Models of inflow-turbulence noise and turbulent-boundary-layer trailing-edge noise are compared to earlier measurements of a 200-kW vertical axis wind turbine so that conclusions regarding the origin of the aerodynamic noise can be drawn. The measurement campaigns, which aimed at establishing the noise emission value and locating the aerodynamic noise sources with a microphone array, are here both compared to further modified versions of the trailing-edge and inflow-turbulence models respectively. Unlike the case for horizontal axis wind turbine, inflow-turbulence noise is deemed as the prevailing noise mechanism. Reducing the self-induced turbulence could then be an effective way of lowering the noise levels for vertical axis wind turbines. Also, looking at the directivity of the inflow-turbulence noise model which indicate most noise in the cross-wind directions, a deviation from the standard downwind measurement position for measuring noise emission is suggested for the VAWT case.

## 1. Introduction

Wind turbines can be categorized by the orientation of their axis of rotation into two groups: horizontal axis wind turbines (HAWTs) and vertical axis wind turbines (VAWTs). From a historical perspective, different sub-concepts of both HAWTs and VAWTs have had individual threads of development in both Europe and North America [1-3]. It was mainly one of these sub-concepts, the upwind 3-bladed HAWT that established itself on the market in the 1970-80s in Denmark, where it thereafter has developed into the large and economically feasible wind turbines of today.

However, the wind turbine industry is today facing several challenges, for example, local environmental impact as well as service cost and reliability. These challenges match some of the possible advantages of the VAWT technology, which has led to a renewed interest in the concept. By using a vertical shaft to transfer the torque, VAWTs can have the generator and other key parts located at ground level which enables designing them with focus on performance and economy rather than size and mass. Furthermore, maintenance and modifications are made easier with these parts placed on the easily accessible tower base. Yaw motors are superfluous since VAWTs are omni-directional, which allows for a design with essentially only one moving part, including blades, struts, shaft and generator rotor which are all jointed. Of special interest here, the concept has shown potential for lower noise emissions, which enables establishment closer to inhabited areas [4, 5]. Moreover, in [6] it has been shown that the



concept is more suitable for up-scaling to  $> 10$  MW than the HAWT concept; it has also been suggested that, mainly due to its low center of mass, it is more suitable for floating off-shore platforms [7].

Noise is considered as one of the disadvantages with wind turbines and noise immissions at dwellings and other sensitive areas is generally regulated in national legislation which restrains potential locations when planning for wind power. Noise from operating wind turbines can be divided into mechanical and aerodynamic noise with the aerodynamic noise being dominant for modern turbines [8]. While the mechanisms behind aerodynamic noise from HAWTs have been thoroughly investigated, the origin of aerodynamic noise from VAWTs is still to a large extent an open question. The work in this paper is a continuation of earlier attempts [4, 5] to understand how VAWT noise is created.

When designing a wind farm, the noise immission are typically simulated based on reported noise emissions of the specific wind turbine model. The noise emission is measured according to the IEC standard [9], which specifies individual procedures for HAWTs and VAWTs respectively. The difference being that for a VAWT, the sound pressure level is measured at a downwind distance  $R_h = H + D$ , which is further away than the  $R_h = H + D/2$  that is stated for HAWTs.

**Table 1.** Properties of the T1-turbine.

Rated power	200 kW
Turbine diameter	26 m
Tower height	38 m
Hub height <sup>1</sup>	41 m
Wing length	24 m
Swept area	624 m <sup>2</sup>
Cut-in wind speed	4 m/s
Rated wind speed	12 m/s
Cut-out wind speed	25 m/s
Survival wind speed	60 m/s
Rotational speed	16-33 rpm
Operational tip speed ratio	3.8
Power regulation	Passive stall
Wing/strut material	Fiberglass composite
Tower material	Laminated Wood



**Figure 1.** The T1-turbine.

### 1.1. The 200-kW VAWT H-rotor

The VAWT we consider in this study is a so called H-rotor, which is a Darrieus-type turbine with straight fixed blades. A 200-kW VAWT (hereafter referred to as the T1-turbine) was erected in 2010 just outside Falkenberg on the Swedish west coast by the company Vertical Wind AB in collaboration with Uppsala University. Only one 200-kW turbine was ever built by Vertical Wind AB, making the T1-turbine unique. This particular VAWT has a direct-drive permanent-magnet synchronous generator which is mounted at the bottom of the tower and connected to the rotor by a steel shaft. The rotor consists of three 24 m long straight blades that are connected to the shaft by two struts each. Both blades and struts are made out of fiberglass. The turbine's blades have a fixed pitch, but the variable speed of operation allows control of the rotor through the stall effect. The aerodynamic power coefficient has been measured to 0.33 [10], and the noise characteristics of the turbine have also been studied [4, 5]. The T1-turbine has a tower made out of laminated wood covered by fiberglass laminate. From the start the tower was free standing, but after two years it was complemented with three guy wires. The construction may

<sup>1</sup> The hub height includes the tower, the small hill covering the generator and half the hub shaft that is carrying the struts.

therefore be described as semi-guy wired [11]. The guy wires were added because small fatigue cracks appeared in some of the glue joints attaching the steel flanges to the glue-laminated wood. A more detailed description of the 200-kW experimental turbine can be found in [12] while a review of Uppsala University's entire work on VAWTs can be found in [13].

## 2. Theory

Aerodynamic noise sources can be divided depending on causation, most notably airfoil self-noise and inflow-turbulence noise. Airfoil self-noise is caused by the interaction between the turbulence created by the blade and the airfoil itself [14]. The airfoil self-noise sub-group turbulent-boundary-layer trailing-edge (TBL-TE) noise is created when the turbulent boundary layer, that develops along the blade surface and convects downstream, passes the trailing edge. The sudden change when the blade surface disappears causes sound to be scattered as broadband noise. In [15], microphone array measurements showed that for a modern HAWT, TBL-TE noise is the dominant noise source. Other airfoil self-noise sub-groups include tip noise, blunt trailing-edge noise, separation-stall noise and laminar-boundary-layer vortex-shedding noise. For more information about these and other sub-groups, well explained descriptions can be found in [8].

The inflow-turbulence noise is created when upstream turbulence interacts with the leading edge of the blade [8]. The sound is caused when the turbulent eddies is scattered at the leading edge, creating noise of broadband character. This noise source is dependent on the amount of incoming turbulence, hence both the atmospheric conditions and the eventual presence of turbulence creating structures in the vicinity, such as other wind turbines, will be of importance. It is to some extent an open issue to what extent inflow-turbulence noise contributes to the overall noise level of a wind turbine [8], although it has been shown that it is not the dominant effect for the large-scale HAWT studied in [15]. However, the contribution of inflow-turbulence noise can be assumed to be greater for VAWTs than HAWTs as the blades are passing in the turbulent wake of the previous passing blades.

### 2.1. TBL-TE noise model

The TBL-TE noise contribution is estimated using the TBL-TE part of the empirical model for airfoil self-noise in [14]. For small VAWTs (low Reynold numbers), laminar-boundary-layer trailing edge noise has been observed to be important [16], but for the larger-sized turbine considered here the Reynolds number is of the order of  $1 \times 10^6$ , so the TBL-TE is expected to be dominant over the laminar-boundary-layer part. A complication is that the model in [14] assumes static angles of attack, whereas in this case the angle of attack is constantly changing. However, static angle-of-attack lift and drag data has been successfully used in prediction models of VAWT performance [17], so it is reasonable to expect that a static approach will be acceptable here as well. The model for the sound pressure level has the following main characteristics [14, 15]:

$$SPL_{\text{TBL-TE}} = 10 \log_{10} \left( \frac{L M^5 \delta^*}{R^2} \frac{\sin^2 \Theta / 2 \sin^2 \Phi}{(1 + M \cos(\Theta + \alpha))^4} \right) + K_1(f), \quad (1)$$

where  $L$  is the blade span,  $M$  is the local Mach number,  $\delta^*$  is the displacement thickness of the boundary layer at the trailing edge,  $R$  is the distance from observer,  $\Theta$  and  $\Phi$  are angles specifying the direction of the observer relative to the blade (see [4]),  $\alpha$  is the angle of attack and  $K_1(f)$  is a frequency dependent constant. The local Mach number and the angle of attack are calculated from a simplified model where the flow is undisturbed by the turbine. The displacement thickness and the constant  $K_1$  are calculated according to the prescription in [14]. Further information about the application of this model to the current geometry is found in [4].

### 2.2. Inflow-turbulence noise model

An important difference between VAWTs and HAWTs with respect to noise generation is that the blades of a VAWT, at the downstream half of the rotation, pass the wake of the blades at the upstream half.

The turbulence levels at the downstream half of a VAWT is then expected to be much larger than the turbulence of the flow ahead of the turbine, due to the upstream blade disturbing the flow. Inflow-turbulence has been proposed to be a significant source of noise even for HAWTs, depending on the turbulence properties of the incoming flow [8]. The flow of a small 2-bladed VAWT was mapped experimentally in [18] where it was observed that a significant amount of turbulence is generated by the blades and struts. The velocity fluctuations appears to be dominated by the tip vortices, but a significant amount of turbulence is also seen to be generated by the struts and the tower, apparently a lot more than the contribution from the trailing-edge vorticity. The turbulence generated by the tower and the struts is indeed observed to collide with the downstream blade path. This means that turbulent inflow might be a potential noise source for VAWTs, irrespective of the atmospheric properties. The model used here builds on [19, 20], and the adaptation to the current geometry is further described in [5]. The main characteristics of the model in the mid frequency range is captured by:

$$SPL_{\text{Turb}} = 10 \log_{10} \left( \frac{L M^{10/3} I^2}{R^2 \ell^{2/3}} \frac{\sin^2 \Theta \sin^2 \Phi}{(1 + M \cos \Theta)^4} \right) + K_2(f), \quad (2)$$

where  $L$  is the blade span along which noise is created,  $I$  is the turbulence intensity,  $\ell$  is the turbulence length scale, and  $K_2(f)$  is a frequency dependent constant, which may be calculated according to the framework given in [5]. Regarding the self-induced turbulence, the noise-generating span  $L$ , as well as the approximate size of the turbulent air stream that is proposed to be originating from the strut-blade joint, is estimated from the microphone-array measurements of [5]. Moreover, the turbulence intensity  $I$  is estimated to be of the order of 0.4 using the an energy extraction argument based on a comparison of  $C_p$  measurements for the current design and strutless designs, see [5]. The turbulence length scale is taken to 0.3 m since that is the length scale of the structure that is proposed to generate the turbulence. In addition to the self-induced turbulence, the current study also includes the ambient turbulence hitting the leading edge of the blades during the whole revolution. The turbulence length scale for this background inflow turbulence is taken to be the height above the ground (40 m), as is conventional [20]; this scale is also indicated by the long term wind measurement used for the noise emission measurement.

### 3. Method

Two separate noise measurements campaigns on the T1-turbine have previously been performed. One noise emission measurement to evaluate the noise levels, and one microphone array measurement aiming to localize aerodynamic noise sources; for details of the measurement setups and data processing, see [4, 5]. The positions for the array measurement setup as well as the emission measurement setup are indicated in Table 2 and Figure 2.

**Table 2:** Wind speed, measurement-position angle, and measured atmospheric turbulence intensity for the measurement positions. The wind direction angle is relative to the measurement-position direction. For the emission (long-term) measurement, the mean and standard deviations are given.

Position	Wind speed at hub height (m/s)	Wind speed at 10 m (m/s)	Measurement-position angle	Turbulence intensity
Array pos 1	4.7	3.7	31°	0.20
Array pos 2	6.0	4.7	126°	0.11
Array pos 3	5.4	4.2	218°	0.12
Array pos 4	5.0	3.9	303°	0.13
Emission meas	8.0 ± 1.7	6.3 ± 1.3	353° ± 10°	0.16

The angle is always relative to the momentary wind direction. Table 2 also displays the measured wind speeds and turbulence intensities. We note that the measured atmospheric turbulence intensities are much lower than the estimated self-induced turbulence intensity at 0.4, (furthermore with a much shorter

length scale) as discussed above. Note also that the mean position during the noise emission measurement is close to, but not exactly, downwind (which would correspond to  $360^\circ$  or  $0^\circ$ ).

In the previous works, results from the noise measurements were compared to a model of the TBL-TE noise and the array measurements were compared to a model of the inflow-turbulence noise. A combined analysis was however not performed. Here, both models are compared simultaneously to the noise emission measurements and the array measurement respectively. Further differences in this study, compared to [4, 5], are (i) that for the comparison of the models to the long-term noise emission measurement, during which time the wind direction fluctuated (quantified in Table 2), the models used here also include averaging the level over a range of wind directions, and (ii) the effect of the atmospheric inflow turbulence is included.

#### 4. Results and discussion

To investigate which noise source is the most important for the T1-turbine, models for the TBL-TE and inflow-turbulence noise are compared with measured results from the noise emission and microphone array campaigns. When comparing the measured results with the models for a certain recording position, the difference in directivity of the two noise contributions will alter the comparison depending on position. Therefore, the directivity of the two models must be considered before drawing conclusions. The directivities as well as marked out recording positions can be seen in Figure 2. Most noise is emitted when the blade is moving toward the wind for both models, and both models show a directivity that, for each blade position, suppresses noise if the observer is behind the blade and precisely in line with the blade chord. (For the inflow-turbulence model, noise is suppressed also at the corresponding position ahead of the blade, see Eq (2).) Summing up the contributions over the whole revolution, however, the inflow-turbulence model shows a sharper directivity pattern, due to the narrow region where the blade interact with self-induced turbulence (while noise is created more evenly during the entire revolution for the TBL-TE model). The dip in the noise level from the inflow-turbulence model is at the position where the observer is standing in line with the emitting blade.

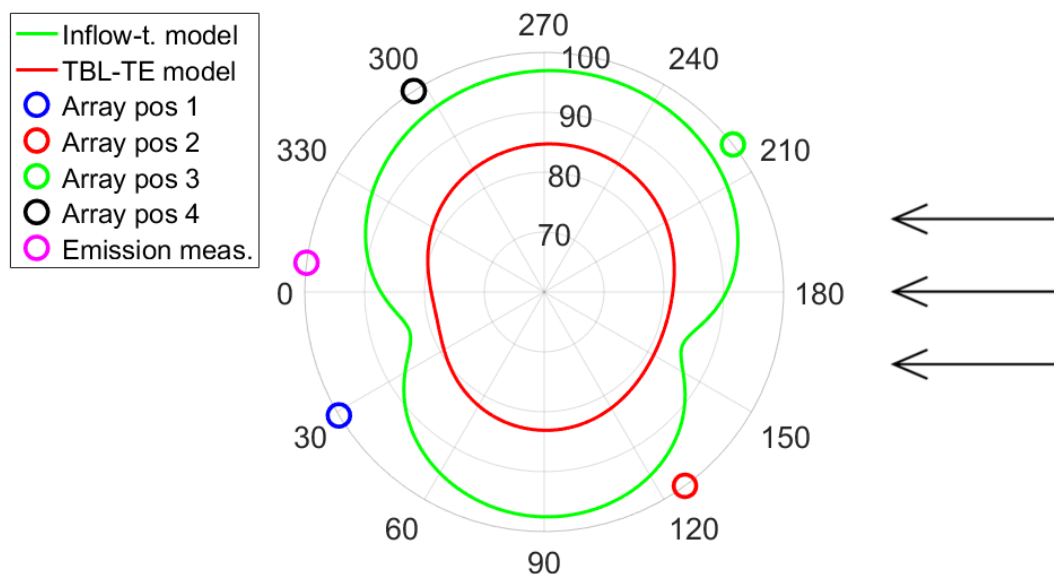


**Figure 2.** Directivity of the inflow-turbulence model (green) and TBL-TE model (red) as seen from above with the wind coming in from the right. The comparison is for a distance of 40 m from the turbine base, a wind speed (hub height) of 8.0 m/s (6.3 m/s at 10 m height) and  $n=22$  rpm. The positions (measurement angles) for microphone array measurements and noise emission measurement are marked in the figure. Units in dBA and degrees counted counterclockwise from downwind position.

The noise emission measurement is compared to the models in Table 3 and Figure 3. For both the emission levels and 1/3-octave bands, it is clear that although the levels from both models are substantially lower than the measured levels, the inflow-turbulence model is closer than the TBL-TE model. The still lower levels of the inflow-turbulence model compared to the measured levels could be explained by directivity issues of the models; the directivity seem to have a sharper directivity in the model than in reality (the downwind position is close to where the least noise is expected, see Figure 2). Note that the values in Table 3 relates to integer wind speeds specified at the height 10 m, since noise emission from wind turbines are typically specified at wind speeds at 10 m height. Figure 2 and 3, on the other hand, relates to 8.0 m/s wind speed at hub height (which was the mean wind speed encountered during the noise emission measurement), corresponding to 6.3 m/s at 10 m.

**Table 3:** Measured noise emission and equivalent model values for 40 m downwind of the turbine. The models include averaging of a wind direction range with standard deviation  $10^\circ$ .

Wind speed at 10 m height (m/s)	5	6	7	8
Tip-speed ratio	3.8	3.8	3.4	2.9
Measurement (dBA)	93.1	94.1	95.4	96.2
TBL-TE model (dBA)	73.0	77.8	78.7	78.0
Inflow-turbulence model (dBA)	82.9	88.1	90.7	92.1

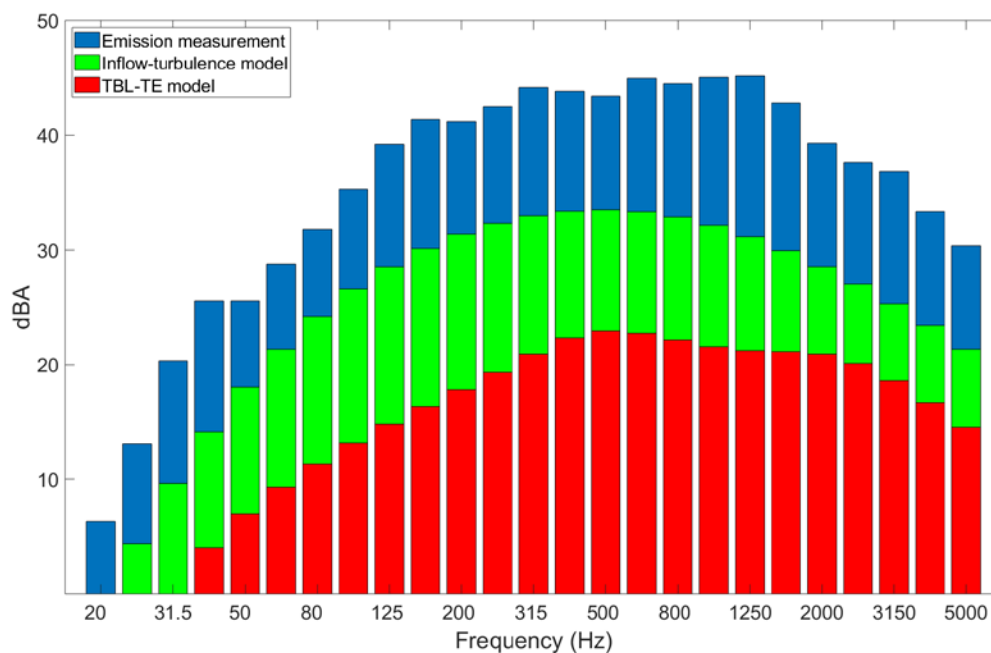


**Figure 3.** Comparison of 1/3-octave band of T1-turbine sound pressure level from noise emission measurements (blue), inflow-turbulence model (green) and TBL-TE model (red). All cases for a wind speed (hub height) of 8.0 m/s (6.3 m/s at 10 m height) and  $n = 22$  rpm. The models include averaging of a wind direction range with standard deviation  $10^\circ$ .

The microphone array measurements are compared to the models in Figure 4, in which the experimental 1/3 octave bands and the corresponding bands from the models can be seen for the four recording positions. For each of the four positions, the wind speed and tip-speed ratio for that specific array recording has been implemented in the models. Overall, the inflow-turbulence model seems to fit better although, for most of the bands, the measured values lie between the two models. The directivity

of both models (see Figure 2) results in low levels for position 1. Although the measured spectrum shows the lowest levels for position 1 (partly explained by the low wind speed during the position 1 recording), the difference compared to the other positions is smaller (apart from the 1000 Hz band). However, the uncertainty in this angle is large, due to varying wind direction and the fact that the wind direction was measured at a mast located 100 m away from the turbine. Moreover, even though it is evident from the results in [5] that most of the noise is created in the exact region handled by the current model, it is clear that some self-induced turbulence exists also behind the hub and the upwind blades in general, which hits the down-wind blade. The lower local wind speed (both where the turbulence is created and where it hits the downwind blade) will produce lower noise levels, but the directivity will be different to the modeled contribution and could possibly be of relevance when the directivity suppresses the dominant contribution. The ambient atmospheric turbulence, which is included in the current model, has a less prominent directivity as noise is created during the whole revolution. However, due mainly to the much longer length scale, this contribution only accounts for some 3 dB at position 1 (and much less for the other positions). It is clear that the inflow-turbulence model, as formulated here, needs to be extended to be able to adequately handle downwind positions.

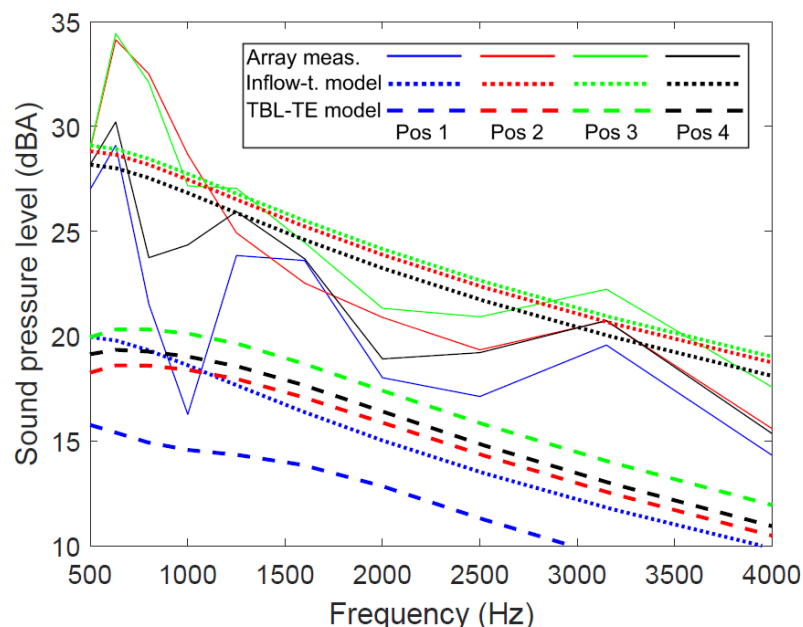


**Figure 4.** Comparison of 1/3 octave band of T1-turbine sound pressure level from inflow-turbulence model (dotted) and TBL-TE model (dashed) as well as the microphone array measurement (solid). For each position, the wind speed used for modelling was the same as during microphone array recording. No averaging over wind directions are done here since this is short-term measurement.

The comparison between the two models, the noise emission measurement and the microphone array measurements indicate that inflow-turbulence noise is the prevailing noise source for the T1-turbine. It seems like the noise produced by the T1 turbine is due to turbulent inflow that is created by the turbine itself, and creating this turbulence in turn degrades the power-conversion performance of the turbine, as discussed in [5]. If it is possible to mitigate the turbulence production in the blade-strut system, this is likely to both enhance the power factor and lower the overall noise level.

The IEC61400-11 standard implies measuring noise emission from a VAWT at a downwind distance  $R_h = H + D$ , which is a longer distance than the  $R_h = H + D/2$  that is implied for HAWTs. This is probably the case because of the distance to the blade at its closest position will be approximately the same in both cases. However, as the most noise seem to be generated when the oncoming blade moves in the opposite wind direction and thus is at a tower distance from the downwind observer, using the

same recording distance for VAWTs as for HAWTs seem to be more reasonable. Additionally, the indicated noise directivity with relatively low levels for the downwind position suggests that a cross-wind direction would be more appropriate when measuring noise emission from VAWTs. Specifying a crosswind direction, it is reasonable to actually keep the longer distance  $R_h = H + D$ , provided that the measurement is done on the side where the blade moves toward the wind.

## 5. Conclusions

Comparing results from the noise emission and the microphone array measurements with models of TBL-TE and inflow-turbulence noise respectively, it is suggested that the inflow-turbulence noise is the prevailing noise mechanism. Reducing the self-induced turbulence could then be an effective way of lowering the noise levels for VAWTs. Regarding the standard for measuring noise emission, it is suggested that the noise should be measured at the cross-wind direction where the blade move toward the wind.

## References

- [1] Gipe P. Wind Energy for the Rest of Us: A Comprehensive Guide to Wind Power and How to Use It. Bakersfield, CA, USA: Wind-Works.Org, 2016.
- [2] Musgrove P. Wind Power. Cambridge, UK: Cambridge University Press, 2010.
- [3] Möllerström E, Gipe P, Beurskens J, Ottermo F. A historical review of installed vertical axis wind turbines rated 100 kW and above. *Renewable and Sustainable Energy Reviews*. 2019;105:1-13.
- [4] Möllerström E, Ottermo F, Hylander J, Bernhoff H. Noise emission of a 200 kW vertical axis wind turbine. *Energies*. 2016;9(1):19.
- [5] Ottermo F, Möllerström E, Nordborg A, Hylander J, Bernhoff H. Location of aerodynamic noise sources from a 200kW vertical-axis wind turbine. *Journal of Sound and Vibration*. 2017;400:154-66.
- [6] Ottermo F, Bernhoff H. An upper size of vertical axis wind turbines. *Wind Energy*. 2013;17(10):1623-9.
- [7] Borg M, Shires A, Collu M. Offshore floating vertical axis wind turbines, dynamics modelling state of the art. Part I: aerodynamics. *Renewable and Sustainable Energy Reviews*. 2014;39:1214-25.
- [8] Bowdler D, Leventhall HG. Wind Turbine Noise: Multi Science Publishing Company, Limited, 2011.
- [9] IEC 61400-11: Wind turbine generator systems—Part 11: Acoustic noise measurement techniques, Edition 3. Geneva, Switzerland: The International Electrotechnical Commission (IEC); 2012.
- [10] Möllerström E, Ottermo F, Goude A, Eriksson S, Hylander J, Bernhoff H. Turbulence influence on wind energy extraction for a medium size vertical axis wind turbine. *Wind Energy*. 2016.
- [11] Möllerström E, Ottermo F, Hylander J, Bernhoff H. Eigen Frequencies of A Vertical Axis Wind Turbine Tower Made of Laminated Wood and the Effect Upon Attaching Guy Wires. *Wind Engineering*. 2014;38(3):277-90.
- [12] Möllerström E. Noise, eigenfrequencies and turbulence behavior of a 200 kW H-rotor vertical axis wind turbine [Ph.D. thesis]: Uppsala University, 2017.
- [13] Apelfröjd S, Eriksson S, Bernhoff H. A Review of Research on Large Scale Modern Vertical Axis Wind Turbines at Uppsala University. *Energies*. 2016;9(7):570.
- [14] Brooks TF, Pope DS, Marcolini MA. Airfoil self-noise and prediction: National Aeronautics and Space Administration, Office of Management, Scientific and Technical Information Division, 1989.
- [15] Oerlemans S, Sijtsma P, Méndez López B. Location and quantification of noise sources on a wind turbine. *Journal of Sound and Vibration*. 2007;299(4–5):869-83.
- [16] Pearson C. Vertical axis wind turbine acoustics [Ph.D. thesis]: Cambridge University, 2014.
- [17] Paraschivoiu I. Wind turbine design: with emphasis on Darrieus concept. Montreal, Canada: Presses inter Polytechnique, 2002.
- [18] Tescione G, Ragni D, He C, Ferreira CS, Van Bussel G. Near wake flow analysis of a vertical axis wind turbine by stereoscopic particle image velocimetry. *Renewable Energy*. 2014;70:47-61.

[19] Paterson R, Amiet R. Acoustic radiation and surface pressure characteristics of an airfoil due to incident turbulence. 3rd Aeroacoustics Conference 1976.

[20] Buck S, Oerlemans S, Palo S. Experimental validation of a wind turbine turbulent inflow noise prediction code. 22nd AIAA/CEAS Aeroacoustics Conference. Lyon, France 2016.